Journal of Sound and Vibration (2002) **255**(5), 867–881
doi:10.1006/jsvi.2001.4190, available online at http://www.idealibrary.com on IDEAL®

DYNAMIC DEM MODEL OF MULTI-SPANS ROTOR SYSTEM

M. YAN AND K. ZHANG

Room 310, *Building* 32, *Department of Mechanics and Engineering Science*, *Peking University*, *Beijing* 100871, *People's Republic of China. E-mails*: *yanmin55@sina.com*; *mechzkk@sina.com*

AND

Y. CHEN

Department of Mechanics, *Tianjin University*, *Tianjin*, 300072, *People's Republic of China*

(*Received* 11 *May* 2001, *and in final form* 12 *December* 2001)

In this paper, the DEM is introduced for the investigation of non-linear dynamical behavior of rotor systems. The modelling procedure and constitutive relations were explained in detail. This model may be used for most of the dynamical problems of rotor systems, such as rub-impacting, bending vibration, torsional vibration, etc. It is especially suitable for studying the rub-impacting problem of rotor system due to the consideration of variable characteristic of friction force with time.

1. INTRODUCTION

A rotor system consists of rotors, bearings, oil film, supports and other parts, which can come into contact with the rotors in motion. Turbine generator set, gas turbine, centrifugal compressor and other kinds of large rotating machines are all typical high-speed ones.

As we know, abnormal vibration in a rotor system can often cause severe accidents [1]. Since Jeffcott began to study dynamic behavior of rotor system by using a single-disk deflective rotor model in the early 20th century [2], one of the problems to which maximum attention is always paid is how to set up the dynamic model of a rotor system. There is no doubt now that many non-linear factors have considerable influence on the local and global dynamic characteristics of a rotor system [3–5]. For example, if deflective deformation or whirling amplitude of a rotor surpasses a certain value in procession, some of its parts will come into contact with and impact those adjacent ones, which are habitually called "rub-impacting". As concerned with many complicated factors, continual rub-impacting will lead to energy transfer and accumulation from rotation to elastic deformation, and it may even cause a sudden breakdown of the rotor. However, these are the factors which make theoritical study and numerical simulation on rub-impacting difficult to deal with, especially in terms of about setting up its dynamic model. One of these factors is that the following characteristics of a rotor system are determined by a series of initial conditions such as whether there is an occurrence of rub-impacting or not, initial location of rub-impacting, values of rub-impacting force and friction force and relations between them, and so on. Another is that the rotor sometimes comes into contacts with and sometimes departs from other adjacent parts, making the occurrence of rub-impacting random and

0022-460X/02/$35.00

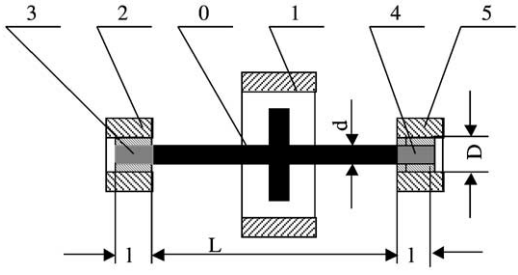

Figure 1. Rotor system: 0, rotor; 1, case; 2, left bearing; 3, left shaft neck; 4, right shaft neck; 5, right bearing.

difficult to decide. In spite of a lot of present research on rub-impacting [1], it needs further study including study of the non-linear method [6, 7]. Therefore, we attempt to carry out some further research on complicated dynamic behavior of rotor system by building a better dynamic model through discrete element method (DEM) [8].

1.1. DEM BRIEF INTRODUCTION

DEM was first referred to as a new numerical method, to study the mechanical behavior of discrete bodies by Cundall in 1971 [8–10], which is especially suitable for simulation of contacting and impacting between discrete bodies as a group. Unlike finite element method (FEM) based on least potential energy variation principle (LPEVP), DEM is based on Newton's Second Law (NSL). For example, we consider a discrete bodies group as a single one, one of them will always be compelled to deform and more under join forces and moments of its adjacent partners. According to NSL with different constitutive relations between bodies, their explicit equations of equilibrium can be set up and they are resolved using the method of difference and iterative computation. Then mechanical parameters of each body such as force field, displacement field, velocity field and so forth can be displayed vividly in the form of computer animation without limitation on the number of bodies.

2. DYNAMIC DEM MODELLING OF ROTOR SYSTEM

Figure 1 shows the diagram of a single-span rotor system, with respect to which DEM dynamic modelling process and concerned computation are as follows.

2.1. DIVIDING UNITS

According to its characteristic based on DEM, the rotor system can be divided into six parts such as rotor, case, left bearing, left shaft neck, right bearing and right shaft neck, which are, respectively, numbered as 0, 1, 2, 3, 4 and 5 as Figure 1 shows.

2.2. MECHANICAL MODEL

2.2.1. *Mechanical model*

Figure 2 shows the DEM dynamic model of a rotor system and constitutive relations between its parts, where we assume that the neck and the bearing has the same constitutive

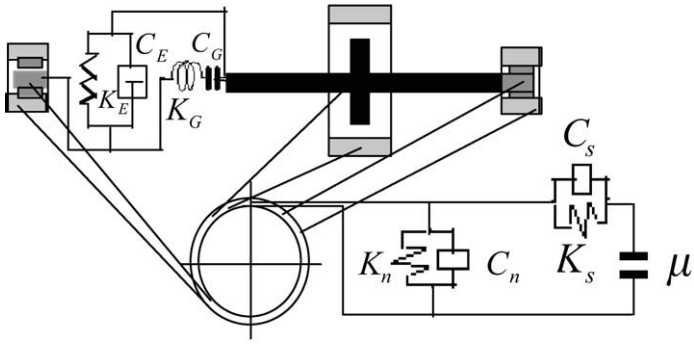

Figure 2. Mechanical model and constitutive relations.

relation as that between the rotor and the case, and both can be simplified into a combination consisting of a normal spring damper K_n–C_n, a tangent one K_s–C_s and a tangent friction slider μ. It must be pointed out that the K_s–C_s works close together with μ: if the tangent force is larger than the friction force between either of the two above-mentioned parts, μ will work and K_s–C_s will not because of the relative sliding movement between them; or else K_s–C_s will work and μ will not. Furthermore, considering the shaft neck and bearing, if the least oil clearance is equal to or larger than zero, then the oil film will not be destroyed, K_n–C_n and K_s–C_s will be fixed by the oil film force while μ is equal to zero; or else such parameters will be calculated according to concrete conditions using a certain method which will be referred to. And the constitutive relation between shaft neck and rotor will be simplified into a spring damper K_E–C_E and a torsion-spring damper K_G–K_G, where the former represents the transverse bending vibration of rotor and the latter torsion vibration.

From the above simplifying process, it can be learned that DEM rub-impacting modelling of rotor system first involves abstracting each part as "disks" and then replacing relations between "disks" with actual constitutive relations.

2.2.2. *Parameters determination*

As Figure 2 shows, rub-impacting will occur when any two parts contact with each other, the effect of which between the two can be explained with a simple combination consisting of a spring damper and a friction slider. The determination of concerned parameters is as follows.

2.2.2.1. *Determination of stiffness parameters.* Considering two inner contact disks as in Figure 3, we can take the boundary area of the larger as being made up of points which lie in the contact area between the smaller and another one that has the same radius that of as the larger s but moves on the orbit with double its radius from the center point of the previous one. Then as Hertz Contact Theory (HCT) [11–14] states the relation of normal force F_n and normal deformation S_n between the two disks can be obtained according to elasticity theory under the assumption that the two have geometric similarity, elasticity similarity, isotropy and are in contact with each other with small strain.

$$F_n = \frac{4}{3}\left[\frac{E_1 E_2}{(1-v_1^2)E_2 + (1-v_2^2)E_1}\right]\left[\frac{r_1 r_2}{r_1 + r_2}\right]^{1/2} S_n^{3/2}, \tag{1}$$

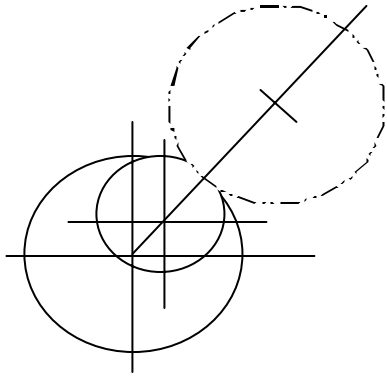

Figure 3. Elements contact transform.

where r_i, v_i and E_i $(i = 1, 2)$ are, respectively, radius, the Poisson ratio and elasticity modulus. Obviously, it is a non-linear function.

Another form of equation (1) is

$$K_n = \frac{F_n}{S_n} = \frac{8r}{3(\theta_1 + \theta_2)} \tag{2}$$

where

$$r = \sqrt[3]{3F_n r_1 r_2(\theta_1 + \theta_2)/8(r_1 + r_2)}, \qquad \theta_i = 2(1 - v_i^2)/E_i \tag{3}$$

is the contact radius. Then, the tangent stiffness is

$$K_s = \frac{8r}{(2 - v_1)/G_1 + (2 - v_2)/G_2} \tag{4}$$

where $G_i = E_i/2(1 + v_i)$ is the shear modulus.

As equations (2) and (4) show, the normal stiffness and the tangent stiffness both vary with r which is relative to normal force that is decided by relative normal deformation between two disks. Thus, the first step of DEM is always to judge as to whether two disks are in contact according to the relative normal deformation being positive or negative (positive means contact, and negative means no contact). Then the normal force, normal stiffness, contact radius and tangent stiffness can be calculated in sequence. In the DEM model, we set the normal stiffness and tangent stiffness as being varied which may probably simulate actual non-linear variation with respect to the concerned parameters.

Unlike the normal force, the tangent force has not explicit expression so that its calculation is complicated. Furthermore, it is also related to the friction force caused by relative movement between the disks. So its calculation is always completed with the increment method on the assumption that the tangent force increment ΔF_s is directly proportional to the relative tangent displacement increment ΔS_s in each iteration step, i.e.,

$$\Delta F_s = K_s \cdot \Delta S_s. \tag{5}$$

This means that due to contact between disks, the tangent stiffness is constant in each iteration step but variable in the whole process.

2.2.2.2. *Determination of damping parameters.* The normal viscous damping coefficient C_n between the two related disks can be obtained from impacting recovery coefficient ξ as

$$C_n = -\frac{2\ln(\xi)\sqrt{K_n M}}{\sqrt{\pi^2 + \ln^2(\xi)}}, \qquad M = \frac{m_1 m_2}{m_1 + m_2}, \tag{6}$$

where m_i is the mass of disk i.

From equation (6) we know that C_n is variable in the whole iteration process because normal stiffness, to which C_n is related besides ξ, varies with time and must be recalculated in each time step.

The tangent damping is a certain kind of dissipation performed by the two disks, between which there is not macroscopic relative sliding but microscopic deformation. Therefore, because of its tiny energy loss it can be simplified as

$$C_S = 0. \tag{7}$$

As a whole, it can be said from the above description that DEM is very suitable for simulating the rub-impacting of rotor system.

2.2.2.3. *Parameters determination of the bending and torsion model.* The transverse bending deformation and torsion deformation of rotor system are both performed by spring dampers in DEM model. Their parameters are decided as follows:

(1) *Determination of stiffness coefficients.* In DEM model, the transverse bending deformation and torsion deformation of rotor system are both simulated according to related equivalent law. Because of the limitation of space, there is no detailed discussion.

(2) *Determination of damping coefficients.* Here, damping means a certain kind of dissipation performed by internal resistance of material in the beam because of elastic deformation of bending and/or torsion in vibration. Its coefficients are difficult to determine and can only be fixed through experiments.

2.3. CALCULATION METHOD

2.3.1. *Interaction between units*

For convenience, the elements referred to later are all placed in the first quadrant of the global co-ordinate system o–xyz. The elements i and j are at the location shown in Figure 4 at the time t and their radii are, respectively r_i, r_j. The origin point of their local co-ordinate system O–XYZ is fixed at the center of element i, axis X is through the center points of the two units from i to j, axis Y is parallel to plane x–y through the center of i and in the plane vertical to axis X, axis Z can be decided according to the right-hand rule. Then, we can obtain the corresponding relation of such physical parameters between o–xyz and O–XYZ as relative displacement, relative velocity and reciprocal forces between the elements (some physical parameters may be zero, which are still included in the relation for the universality of the calculation method):

$$\begin{Bmatrix} X \\ Y \\ Z \end{Bmatrix} = [T] \begin{Bmatrix} x \\ y \\ z \end{Bmatrix} \quad \text{or} \quad \begin{Bmatrix} x \\ y \\ z \end{Bmatrix} = [T]^{-1} \begin{Bmatrix} X \\ Y \\ Z \end{Bmatrix} \tag{8}$$

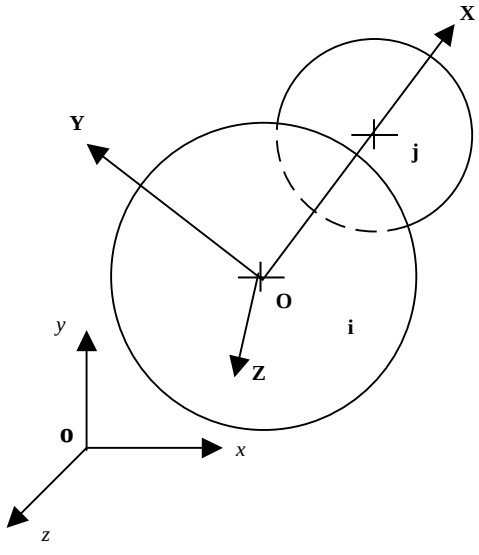

Figure 4. Element position.

where

$$[T] = \begin{Bmatrix} \cos\alpha & \cos\beta & \cos\gamma \\ -\dfrac{\cos\beta}{\sqrt{\cos^2\alpha + \cos^2\beta}} & \dfrac{\cos\alpha}{\sqrt{\cos^2\alpha + \cos^2\beta}} & 0 \\ -\dfrac{\cos\alpha\cos\gamma}{\sqrt{\cos^2\alpha + \cos^2\beta}} & -\dfrac{\cos\beta\cos\gamma}{\sqrt{\cos^2\alpha + \cos^2\beta}} & \sqrt{\cos^2\alpha + \cos^2\beta} \end{Bmatrix} \tag{9}$$

is the transform matrix from o–xyz to O–XYZ. $\cos\alpha$, $\cos\beta$ and $\cos\gamma$ is direction cosine in o–xyz, that is,

$$\cos\alpha = \frac{x_j - x_i}{D_{ij}}, \qquad \cos\beta = \frac{y_j - y_i}{D_{ij}}, \qquad \cos\gamma = \frac{z_j - z_i}{D_{ij}} = 0, \tag{10}$$

where

$$D_{ij} = \sqrt{(x_j - x_j)^2 + (y_j - y_i)^2 + (z_j - z_j)^2}. \tag{11}$$

During the period of the Δt, displacement increment and the angle increment of i and j are, respectively,

$$\begin{gathered} \Delta u_{xi} = \dot{x}_i \Delta t, \quad \Delta u_{yi} = \dot{y}_i \Delta t, \quad \Delta u_{zi} = \dot{z}_i \Delta t = 0, \\ \Delta\varphi_{xi} = \dot{\varphi}_{xi}\Delta t = 0, \quad \Delta\varphi_{yi} = \dot{\varphi}_{yi}\Delta t = 0, \quad \Delta\varphi_{zi} = \dot{\varphi}_{zi}\Delta t, \\ \Delta u_{xj} = \dot{x}_j \Delta t, \quad \Delta u_{yj} = \dot{y}_j \Delta t, \quad \Delta u_{zi} = \dot{z}_j \Delta t = 0, \\ \Delta\varphi_{xj} = \dot{\varphi}_{xj}\Delta t = 0, \quad \Delta\varphi_{yj} = \dot{\varphi}_{yj}\Delta t = 0, \quad \Delta\varphi_{zj} = \dot{\varphi}_j \Delta t. \end{gathered} \tag{12}$$

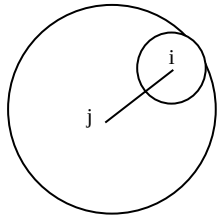

Figure 5. Rub-impact.

Therefore, we can obtain the angle and displacement of i relative to j in O–XYZ.

$$\begin{Bmatrix} \Delta\varphi_X \\ \Delta\varphi_Y \\ \Delta\varphi_Z \end{Bmatrix} = [T] \begin{Bmatrix} \Delta\varphi_{xi} - \Delta\varphi_{xj} \\ \Delta\varphi_{yi} - \Delta\varphi_{yj} \\ \Delta\varphi_{zi} - \Delta\varphi_{zj} \end{Bmatrix} \tag{13}$$

$$\begin{Bmatrix} \Delta u_X \\ \Delta u_Y \\ \Delta u_Z \end{Bmatrix} = [T] \begin{Bmatrix} \Delta u_{xi} - \Delta u_{xj} \\ \Delta u_{yi} - \Delta u_{yj} \\ \Delta u_{zi} - \Delta u_{zj} \end{Bmatrix} + \begin{Bmatrix} 0 & 0 \\ \Delta\varphi_{Zi} & \Delta\varphi_{Zj} \\ -\Delta\varphi_{Yi} & -\Delta\varphi_{Yj} \end{Bmatrix} \begin{Bmatrix} r_i \\ r_j \end{Bmatrix}, \tag{14}$$

where

$$\begin{Bmatrix} \dot{\varphi}_{Xi} \\ \dot{\varphi}_{Yi} \\ \dot{\varphi}_{Zi} \end{Bmatrix} = [T] \begin{Bmatrix} \dot{\varphi}_{xi} \\ \dot{\varphi}_{yi} \\ \dot{\varphi}_{zi} \end{Bmatrix} \quad \begin{Bmatrix} \dot{\varphi}_{Xj} \\ \dot{\varphi}_{Yj} \\ \dot{\varphi}_{Zj} \end{Bmatrix} = [T] \begin{Bmatrix} \dot{\varphi}_{xj} \\ \dot{\varphi}_{yj} \\ \dot{\varphi}_{zj} \end{Bmatrix}, \tag{15}$$

$$\Delta\varphi_{Zi} = \dot{\varphi}_{Zi}\Delta t,\ \Delta\varphi_{Zj} = \Delta\dot{\varphi}\Delta t,\ \Delta\varphi_{Yi} = \Delta\dot{\varphi}_{Yi}\Delta t,\ \Delta\varphi_{Yj} = \Delta\dot{\varphi}_{Yj}\Delta t. \tag{16}$$

As a rule, we take the forward direction of axis as positive relative displacement and counter-clockwise along axis as positive relative angle. Thus, the mutual effect between the elements can be decided as follows:

2.3.1.1. *Rub-impacting forces.* Figure 5 shows a kind of general rub-impacting of rotor system. At the time t, the elements i and j can be considered to be in contact with each other, if

$$D_{ij} = \sqrt{(x_j - x_j)^2 + (y_j - y_i)^2 + (z_j - z_j)^2} > r_j - r_i \tag{17}$$

is satisfied. Then the normal force between them is

$$F_{Xne}^{(t)} = \frac{4}{3}\left[\frac{E_1 E_2}{(1 - v_1^2)E_2 + (1 - v_2^2)E_1}\right]\left[\frac{r_1 r_2}{r_1 + r_2}\right]^{1/2} S_n^{3/2}, \tag{18}$$

where

$$S_n = D_{IJ} + r_i - r_j \tag{19}$$

and the damping force is

$$F_{Xnd}^{(t)} = C_n^{(t)} \Delta u_X / \Delta t \tag{20}$$

and the join normal force is

$$F_{Xn}^{(t)} = F_{Xne}^{(t)} - F_{Xnd}^{(t)}. \tag{21}$$

The tangent force will not be continuous because of the friction, therefore, firstly we must decide whether there is relative sliding between the elements according to Coulomb's Friction Law. If it is true, the tangent force has to be amended with the maximum static friction force. Now, we can obtain the increment of the tangent elastic force and that of the tangent damping force during each time step Δt as

$$\Delta F_{Ye}^{(t)} = K_s^{(t)} \Delta u_Y, \quad \Delta F_{Ze}^{(t)} = K_s^{(t)} \Delta u_Z,$$

$$\Delta F_{Yd}^{(t)} = C_s^{(t)} \Delta u_Y / \Delta t, \quad \Delta F_{Zd}^{(t)} = C_s^{(t)} \Delta u_Z / \Delta t, \tag{22}$$

then the join tangent force and its elastic component at the time t are, respectively,

$$F_{Ye}^{(t)} = F_{Ye}^{(t-\Delta t)} + \Delta F_{Ye}^{(t)}, \quad F_{Ze}^{(t)} = F_{Ze}^{(t-\Delta t)} + \Delta F_{Ze}^{(t)},$$

$$F_Y^{(t)} = F_{Ye}^{(t)} - F_{Yd}^{(t)}, \quad F_Z^{(t)} = F_{Ze}^{(t)} - F_{Zd}^{(t)} \tag{23}$$

and the maximum static friction force can be obtained from Coulomb's Friction Theory as

$$F_C^{(t)} = |F_n^{(t)}| \mu \Lambda \tag{24}$$

where μ is equal to the minor friction coefficient between the two elements. If

$$\sqrt{(F_Y^{(t)})^2 + (F_Z^{(t)})^2} > F_C^{(t)} \tag{25}$$

is satisfied, then there will be relative sliding between the elements, and the tangent force should be corrected to

$$F_Y^{(t)} = F_C^{(t)} \operatorname{sign}(F_Y^{(t)}) \qquad F_Z^{(t)} = F_C^{(t)} \operatorname{sign}(F_Z^{(t)}). \tag{26}$$

2.3.1.2. *Bending forces.* Without considering tangent bending of the rotor, its normal bending force is

$$F_{XnE}^{(t)} = K_{kE} D_{ij} \tag{27}$$

and the normal bending damping force is

$$F_{XEd}^{(t)} = C_E \Delta u_X / \Delta t, \tag{28}$$

where C_E is the bending damping coefficient of the rotor. Then, the join normal force is

$$F_{XE}^{(t)} = F_{XnE} - F_{XEd}^{(t)}. \tag{29}$$

2.3.1.3. *Movement equations.* Now we have to transform the forces being calculated above in local co-ordinate O–XYZ into those in global co-ordinate o-xyz.

Suppose:

In o–xyz, $F_{xi}^{(t)}$, $F_{yi}^{(t)}$, $F_{zi}^{(t)}$ are, respectively, three components of the join forces on element I along x, y, z at the time t, while $M_{xi}^{(t)}$, $M_{yi}^{(t)}$, $M_{zi}^{(t)}$ are, respectively, the components of moments. Then,

$$\begin{Bmatrix} F_{xi}^{(t)} \\ F_{yi}^{(t)} \\ F_{zi}^{(t)} \end{Bmatrix} = \sum [T]^{-1} \begin{Bmatrix} F_{Xni}^{(t)} + F_{XEi}^{(t)} \\ F_{Yi}^{(t)} \\ F_{Zi}^{(t)} \end{Bmatrix} + \begin{Bmatrix} F_{xei}^{(t)} + \sum F_{xoili}^{(t)} \\ F_{yei}^{(t)} + \sum F_{yoili}^{(t)} \\ -m_i g \end{Bmatrix}, \tag{30}$$

$$\begin{Bmatrix} M_{xi}^{(t)} \\ M_{yi}^{(t)} \\ M_{zi}^{(t)} \end{Bmatrix} = r_i \sum [T]^{-1} \begin{Bmatrix} 0 \\ F_{Yi}^{(t)} \\ F_{Zi}^{(t)} \end{Bmatrix} + \begin{Bmatrix} 0 \\ 0 \\ M_{zoili}^{(t)} + \sum M_{Gi}^{(t)} \end{Bmatrix}, \tag{31}$$

where $\sum$ indicates the sum of all the elements which have an effect on element i, $F_{xei}^{(t)}, F_{yei}^{(t)}$ are, respectively, the two components of the exciting force on element i along x, y, accordingly, $F_{xoili}^{(t)}, F_{yoili}^{(t)}$ are the components of the oil film forces; m_i is the mass of element i; g is the acceleration of gravity; $M_{zoili}^{(t)}$ is the moment of oil film forces on element i,

$$M_{Gi}^{(t)} = K_G \Delta\varphi_{Zi} - C_G \Delta\varphi_{Zi}/\Delta t \tag{32}$$

is the moment of the torsion force caused by the torsion deformation of the rotor.

As for determination of the oil film forces, its details it can be obtained from references [15, 16]. Here, it is necessary to point out that any method for calculating discrete oil film forces will be suitable for the model because DEM completes computation during each separate time step, which makes DEM more adaptive for the analysis of rotor system.

Then, at the time $t + \Delta t$, the velocity and angular velocity of element I are, respectively,

$$\begin{Bmatrix} \dot{x}_i^{(t+\Delta t/2)} \\ \dot{y}_i^{(t+\Delta t/2)} \\ \dot{z}_i^{(t+\Delta t/2)} \end{Bmatrix} = \begin{Bmatrix} \dot{x}_i^{(t-\Delta t/2)} \\ \dot{y}_i^{(t-\Delta t/2)} \\ \dot{z}_i^{(t-\Delta t/2)} \end{Bmatrix} + \frac{\Delta t}{m_i} \begin{Bmatrix} F_{xi}^{(t)} \\ F_{yi}^{(t)} \\ F_{zi}^{(t)} \end{Bmatrix}, \tag{33}$$

$$\begin{Bmatrix} \dot{\varphi}_{xi}^{(t+\Delta t/2)} \\ \dot{\varphi}_{yi}^{(t+\Delta t/2)} \\ \dot{\varphi}_{zi}^{(t+\Delta t/2)} \end{Bmatrix} = \begin{Bmatrix} \dot{\varphi}_{xi}^{(t-\Delta t/2)} \\ \dot{\varphi}_{yi}^{(t-\Delta t/2)} \\ \dot{\varphi}_{zi}^{(t-\Delta t/2)} \end{Bmatrix} + \frac{\Delta t}{I_i} \begin{Bmatrix} M_{xi}^{(t)} \\ M_{yi}^{(t)} \\ M_{zi}^{(t)} \end{Bmatrix}, \tag{34}$$

where I_i is the element of inertia of element i. And its displacement and angular displacement at $t + \Delta t$ are

$$\begin{Bmatrix} x_i^{(t+\Delta t)} \\ y_i^{(t+\Delta t)} \\ z_i^{(t+\Delta t)} \end{Bmatrix} = \begin{Bmatrix} x_i^{(t-\Delta t)} \\ y_i^{(t-\Delta t)} \\ z_i^{(t-\Delta t)} \end{Bmatrix} + \begin{Bmatrix} \dot{x}_i^{(t+\Delta t/2)} \\ \dot{y}_i^{(t+\Delta t/2)} \\ \dot{z}_i^{(t+\Delta t/2)} \end{Bmatrix} \Delta t, \tag{35}$$

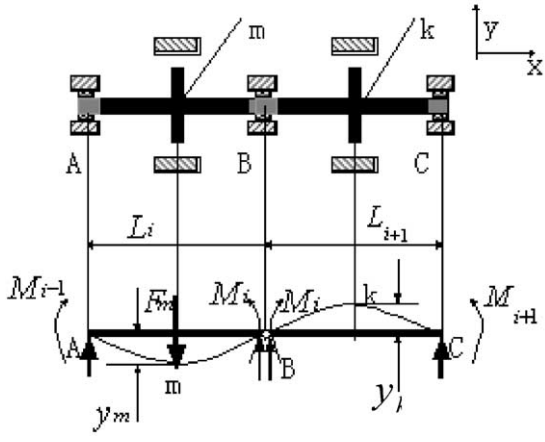

Figure 6. Equivalent stiffness and loads of mult-spans rotor system.

$$\begin{Bmatrix} \varphi_{xi}^{(t+\Delta t/2)} \\ \varphi_{yi}^{(t+\Delta t/2)} \\ \varphi_{zi}^{(t+\Delta t/2)} \end{Bmatrix} = \begin{Bmatrix} \varphi_{xi}^{(t-\Delta t/2)} \\ \varphi_{yi}^{(t-\Delta t/2)} \\ \varphi_{zi}^{(t-\Delta t/2)} \end{Bmatrix} + \begin{Bmatrix} \dot{\varphi}_{xi}^{(t+\Delta t/2)} \\ \dot{\varphi}_{yi}^{(t+\Delta t/2)} \\ \dot{\varphi}_{zi}^{(t+\Delta t/2)} \end{Bmatrix} \Delta t. \tag{36}$$

Now it can begin another iterative calculation in the next time step after re-deciding the effects between the elements.

3. DYNAMIC DEM MODEL OF MULTI-SPANS ROTOR SYSTEM

We will illustrate the dynamic DEM modelling process of multi-spans rotor system with only two of the spans as Figure 6 shows, where A, B and C are bearing points of the rotor system, L_i and L_{i+1} are the respective lengths of AB and BC, m and k are the respective midpoints of AB and BC, M_{i-1}, M_i and M_{i+1} are bending moments acting on points A, B and C, F_m is force acting on point m, y_m and y_k are deflection of points m and k.

Assuming that the joints between the AB span and BC span are continuous, the whole rotor can be regarded as a statically indeterminate and continuous beam and can be divided into several single-span ones with three-moment equations in structure mechanics. Thus, there is no fundamental difference between multi-spans rotor system and single-span one on DEM modelling and calculation. However, we must have cognizance of two basic problems on modelling of a multi-spans rotor system: when dividing multi-spans into singles, one problem is that the bending stiffness of multi-spans beam has changed after division because of surplus supports' action; the other is that part of the deformation of a certain span is caused by load acting on other spans. Therefore, the former requires computation of equivalent stiffness and the latter requires equivalent loads, and then we can begin the next DEM calculation with the above-mentioned method.

4. EXPERIMENT CONTRAST STUDY OF THE NON-LINEAR DYNAMIC DEM MODEL OF ROTOR SYSTEM

From the above discussion, which included a brief introduction of DEM, primary suppose, constitutive relations, dynamic DEM modeling of rotor system and calculation

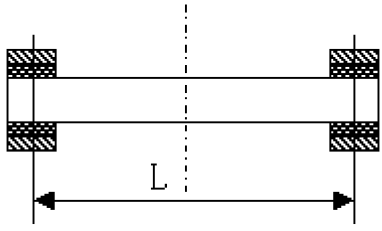

Figure 7. Bearing of rotor.

process, dynamic DEM model of multi-spans rotor system and calculation, it can be learned how to apply the DEM model to the study of non-linear dynamic behavior of rotor system. Contrasting with the results of experiment, all calculation results in this thesis come out from the program based on DEM Model, where the oil film model was obtained from reference [16, 63–67]. In the experimental model obtained from reference [17], to ensure comparability, the structural size and the working conditions of the rotor system are all fixed according to the parameters in reference [17].

4.1. EXPERIMENTAL MODEL

According to reference [17], the experimental model belongs to Jeffocott's rotor system considering oil film force. As Figure 7 shows, the primary parameters include

- *rotor* $r = 40$ mm, radius; $M = 16{\cdot}69$ kg, mass.
- *bearing* $D = 80$ mm, diameter; $L_r = 16$ mm: length of bearing; $L = 280$ mm; distance between the bearing; $C = 0{\cdot}25$ mm, clearance of bearing.
- *parameters of sliding system*: $\mu = 1{\cdot}76\text{e}{-2}$ Pa s, viscidity of the lubricating oil at 50°C; $P = 2{\cdot}0\text{e}{-4}$ Pa, pressure of oil supply.
- *imbalance parameters of rotor*: $M_u = 11{\cdot}54\text{e}{-3}$ kg, eccentric mass; $ru = 6{\cdot}15\text{e}{-2}$ mm, eccentric distance.

For more detailed conditions, refer to reference [17].

4.2. EXPERIMENTAL RESULTS

Figure 8 shows the experimental results of the axes trace and attractor in reference [17], where n indicates the rotating speed of the rotor, whose unit is rounds/min (r.p.m). The conclusion is

(1) At relatively low rotating speed ($3000 \leqslant n \leqslant 4600$ r.p.m), the trace of the rotor's axes is Period-1.
(2) At higher rotating speed, the trace of the rotor's axes is chaos before coming back to Period-1 trace. For example, when $n = 6200$ r.p.m, the attractor of the rotor's axes is a strange attractor.
(3) When $n = 4600$ r.p.m, the trace of the rotor's axes is Period-2.

4.3. CALCULATION RESULTS OF DYNAMIC DEM MODEL [18, 19]

Figures 9 and 10 show the calculation results of the experimental model provided in paper [17], by using Dynamic DEM Model built in this paper. This has no special

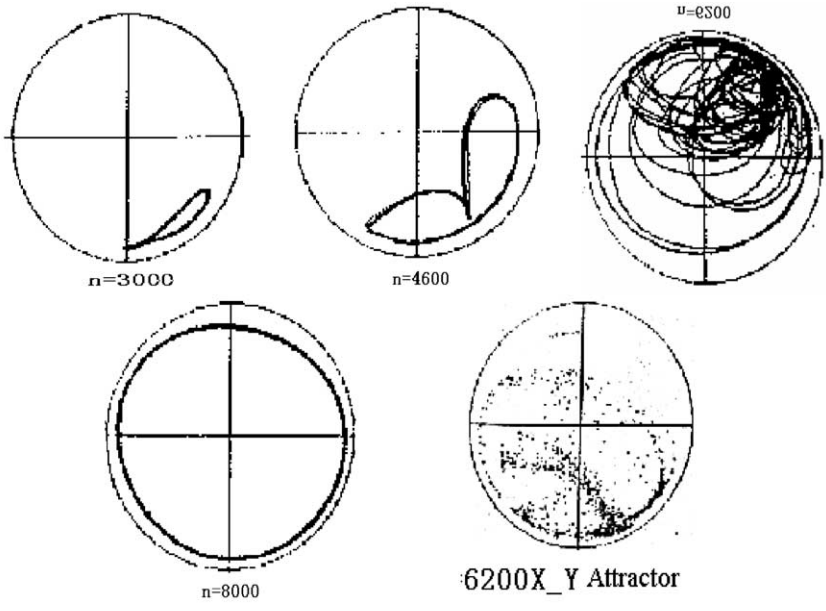

Figure 8. Experimental results of reference [15].

illustration and normally shows the trace of the rotor's axes, where n is the rotating speed with unit rounds/min. It can be obtained from Figures 9 and 10 that:

(1) When ($0 < n < 3980$ r.p.m), the trace of the rotor's axes is Period-1, as $n = 3000$ r.p.m.
(2) When ($3980 \leqslant n < 4940$ r.p.m), the trace of the rotor's axes is Period-2, as $n = 4600$ r.p.m.
(3) When ($4940 \leqslant n < 5360$ r.p.m), the trace of the rotor's axes is Period-1 again, as $n = 5000$ r.p.m.
(4) When ($5360 \leqslant n \leqslant 5870$ r.p.m), the trace of the rotor's axes is quasi-period. For example, when $n = 5400$ and 5800 r.p.m, we can see that the attractor is a closed curve and its shape varies with the rotating speed. In Figure 9, the low-colored curve is Poincare' section of the trace of the rotor's axes in plane X–Y.
(5) When ($5870 < n < 6083$ r.p.m), the trace of the rotor's axes is Period-5. For example, when $n = 6000$ r.p.m, the attractor in plane X–Y has five points.
(6) When ($n \geqslant 6083$ r.p.m), the trace of the rotor's axes is chaos before coming back to quasi-period or period. For example, when $n = 6083$ r.p.m, attractor of the trace of the rotor's axes is a strange attractor and distributing in a certain field. When $n = 8000$ r.p.m, the attractor is also a strange attractor, but its shape is a closed curve, so the movement is quasi-period.
(7) When the dynamic parameters of the rotor system are changed, the movement of the rotor will change significantly, especially when parameters of the sliding bearing are changed. See the case $n = 6500$ r.p.m, the figure shows the attractors in different planes after parameters of the sliding bearing in experimental model are changed, where x' and y' are the speeds in directions X and Y respectively. In $n = 6500$ P_X_X' P_Y_Y' attractor, the left is P_Y_Y' attractor. We can see that the shape of the attractor changed significantly after the parameters changed.

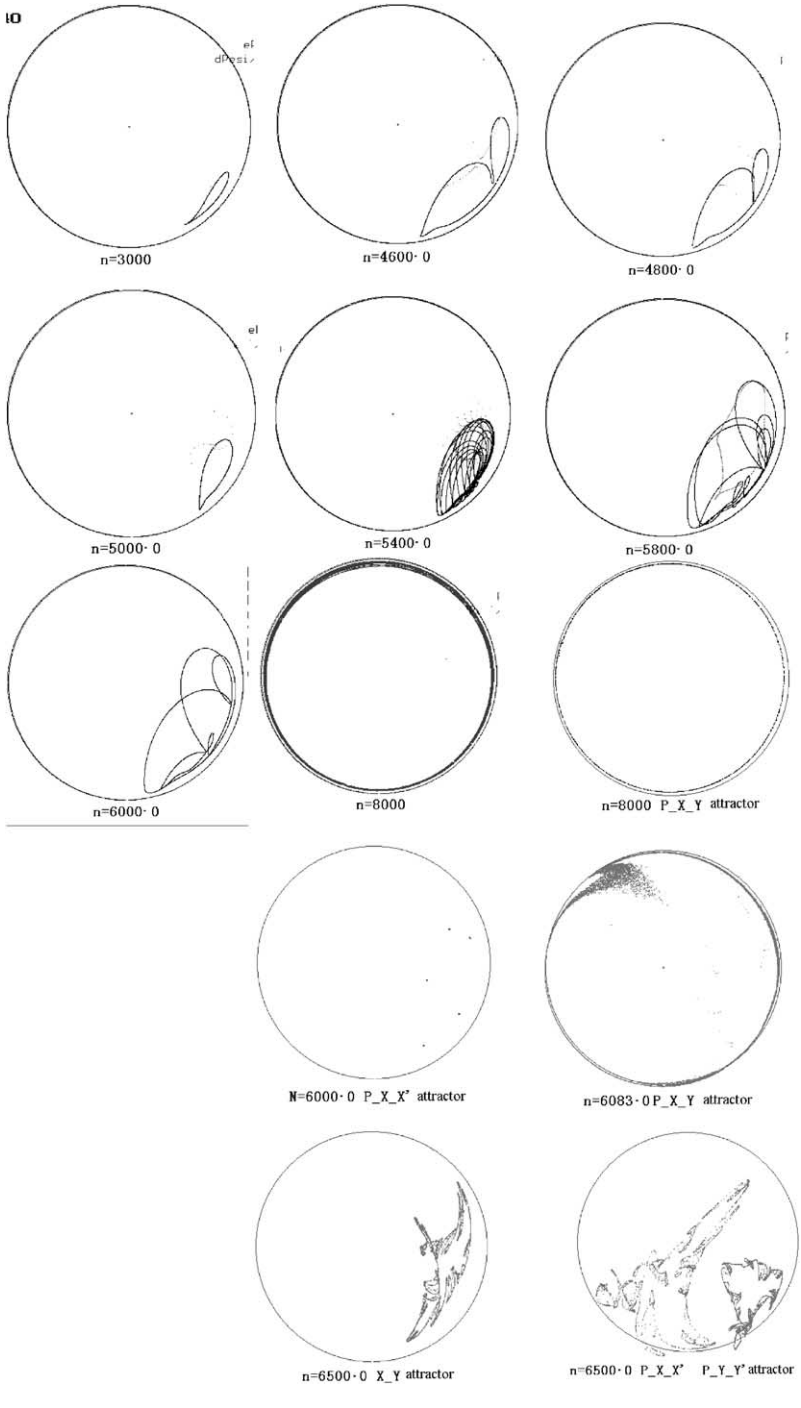

Figure 9. Calculation results of DEM model.

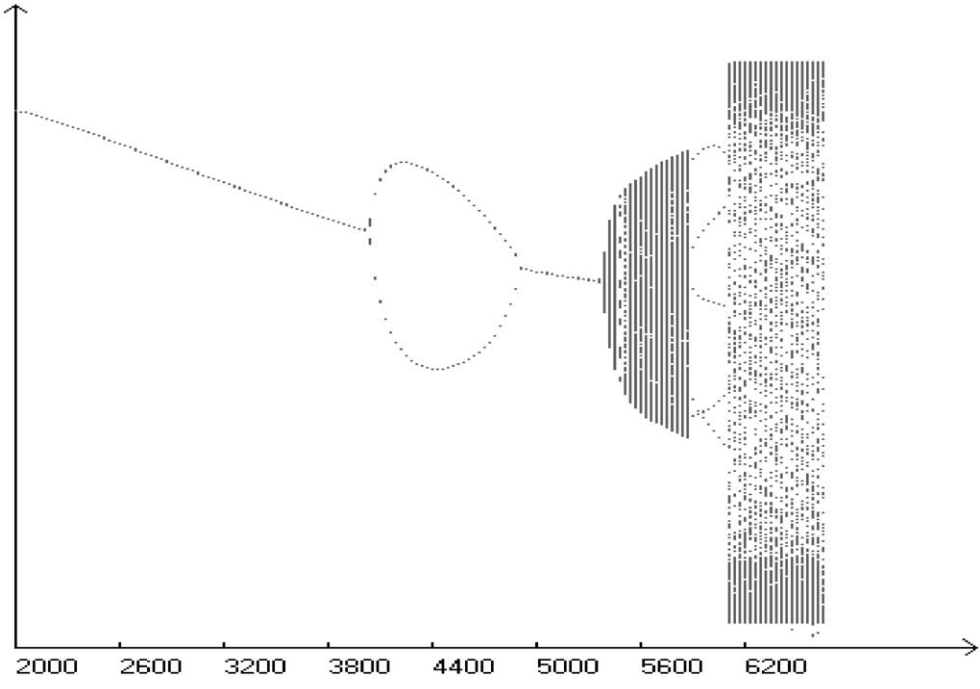

Figure 10. Bifurcation graph.

5. DISCUSSION AND CONCLUSION

(1) After a great deal of calculation on the DEM model of rotor system built in this paper, we find that our results are almost accordant to the experimental results from reference [17] in nature: it can be said that DEM is suitable for calculation on rotor system and our model is reliable.

(2) The dynamic behavior of the rotor shows a strong non-linear tendency before the occurrence of rub-impacting, for instance, the movement rule of the rotor calculated in this paper is: Period-1 → Period-2 → quasi-period → Period-5 → chaos → quasi-period. So the trace of axis of rotor shows strong non-linear characteristics, which is the outcome of liquid quality of the oil film of sliding bearing.

(3) Calculation results on rub-impacting with our DEM model of rotor system can simulate actual rub-impacting more practically, reliably and flexibly, because:
   (1) It adopts non-linear rub-impacting constitutive relation on Hertz Contact Theory.
   (2) Tangent forces varying with time in each time step Δt are calculated based on Coulomb Friction Theory.
   (3) Difficult and random problems, such as whether and where rub-impacting occurs, to what degree it is, what its characteristics are, and so on, are resolved by computer programs automatically.

(4) After obtaining concerned parameters in quantity such as displacements of each support center, displacements of rotor center in each span, relative angle between the elements, and the oil film force, we can decide the bending and torsion of the rotor and the torsion of bearings at all. That is, we can apply DEM to verify the intensity, stiffness and the life of the rotor or bearings.

(5) As the movements and forces of rotor system can be fixed in quantity and simulated in the form of computer animation, therefore, DEM is suitable for determining complicated dynamic behavior of the rotor system as well as designing initial analysis, calculation and display.

(6) Both single-span and multi-span dynamic rotor system can be calculated with our DEM model. Furthermore, we can calculate many kinds of complicated dynamic behavior of a rotor system with many non-linear factors. Therefore, without the limitation of DOF, the DEM model provides a feasible numerical method for the analysis of high dimensional and complicated dynamic rotor system.

REFERENCES

1. W. HUANG 2000 *Journal of Vibration Engineering* **13**, 497–509. Reviews of nonlinear rotor dynamics (in Chinese).
2. H. H. JEFFCOTT 1919 *Philosophical Magazine* **37**, 304–314. The lateral vibration of loaded shafts in the neighborhood of a whirling speed—the effect of want of balance.
3. S. T. NOAH, P. SUNDARARAJAN 1995 *Journal of Vibration and Control* **1**, 431–458. Significance of considering nonlinear effects in predicting the dynamic behavior of rotating machinery.
4. Q. DING 1997 *Ph.D. Thesis*, *Tianjin University*. Study on mechanism subharmonic instability of nonlinear rotor/bearing systems.
5. Z. FU 1999 *Ph.D. Thesis*, *North China Electric Power University*. The theoretical and experimental research on characteristic of coupling flexural—torsional vibration of turbogenerator shafts.
6. Y. CHEN and Q. DING 1998 *Proceedings ICVE*, *Dalian*, 36–39. Some problems on the study of nonlinear dynamics of large scale rotor system.
7. Y. CHEN and Q. DING 1999 *Proceedings DYMAC*99, *Manchester*, *England*, Chapter 87, 395–398. C-L method and its application to subhar monic vibration of nonlinear rotor systems.
8. M. YAN 1990 *Ph.D. Thesis*, *Xi'an University of Technology*. Research and application on characteristics of the vibration ball and laws of the grinding media charges using DEM.
9. Q. WEI 1990 *Ph.D. Thesis. Tsinghua University*. The basic principles, numerical schemes and experimental researches of discrete element method in geotechnical engineering.
10. W. LI 1997 *Xi'an Jiaotong University*. Research and application of theory of impact damping using DEM.
11. S. P. TIMOSKENKO and J. N. GOODIER 1970 *Theory of Elasticity*, 409–422. New York: McGraw-Hill.
12. A. D. DE PATER and J. J. KALKER 1975 *The Mechanics of the Contact Between Deformable Bodies*. Delft: Delft University Press.
13. G. M. L. GLADWELL 1980 *Contact Problems in the Classical Theory of Elasticity*. The Netherlands.
14. K. L. JOHNSON 1985 *Contact Mechanics*. Cambridge: Cambridge University Press.
15. W. ZHANG, S. CUI, X. XU and H. ZHANG 2000 *An General Mathematical Model of Nonlinear Oil-Film Forces for Bearings with Unsteady Perturbed Motioned. Advances in Engineering Mechanics*. Peking: Peking University Press.
16. Y. ZHONG 1987 *Rotor Dynamics*, 63–67. Tsinghua: Tsinghua University Press.
17. G. ADILETTA, A. R. GUIDO and C. ROSSI 1997 *Nonlinear Dynamics* **14**, 157–189. Nonlinear dynamics of a rigid unbalanced rotor in journal bearings. Part II: experimental analysis.
18. S. ZHANG and Q. LU 2000 *Acta Mechanica Sinica* **32**, 59–69. A nonsmooth analysis on the rub-impacting rotor system (in Chinese).
19. Y. CHEN 1993 *Bifurcation and Chaos Theory of Nonlinear Vibration Systems*. Beijing: Higher Education Press.